MEASURING LUNG ABNORMALITIES IN IMAGES-BASED CT

A. Lay-Ekuakille*[1], P. Vergallo[2], I. Jabłoński[3§], S. Casciaro[4#] and F. Conversano[5#]

Department of Innovation Engineering, University of Salento,73100, Lecce, Italy

§ Chair of Electronic and Photonic Metrology, Wrocław University of Technology, Poland

National Council of Research, Institute of Clinical Physiology, 73100 Lecce, Italy.

Email: aime.lay.ekuakille@unisalento.it

Submitted: Dec. 14, 2015 ***Accepted: Apr. 1, 2016*** ***Published: June 1, 2016***

Abstract - Diagnosis by imaging is one of the most important findings in biomedical imaging because it allows not only the diagnosing of a specific pathology but to perform online and offline surgical operations using imaging as it is noticed in interventional radiology. This paper illustrates the use Hough transform in identifying pathological structures included in CT (Computer Tomography) and HRCT (High Resolution Computer Tomography) images related to patients suffering from lung disease. These abnormal areas appear as bulges of the trophic vessels and they are similar to circular structures with level of lighter gray near to white. Circular Hough transform (CHT) identifies regions with a circular shape. However, a metrics is defined in order to understand if the pointed out area has a pathological morphology. CHT is used here for helping to detect possible events of indolent tumors or undetermined significance pathologies for lung apparatus. For this aim, we use entropy approach with CHT because it measures the scatter of the directional elements in an image. In fact a high entropy value is related to areas with a strong contrast in grayscale, and abnormalities in the image are present as a set of points with more lighter than the dark background. The results have shown, by means of an accuracy true table, rendering a comparison between clinicians'diagnosis and CHT detection, it is possible to indicate, with a better accuracy, potential areas of undetermined significance pathologies. Finally, a receiver operational curve (ROC) is used as an accuracy index for evaluating the positive impact of entropy on diagnosis.

Index terms: Hough and Radon transform; Biomedical imaging; Computer tomography detection accuracy; Indolent tumor; Receiver operational curve.

I. INTRODUCTION

Biomedical image is a kind of measurement signal of observations and transformation that brings to new conclusion about object, giving new facts and indicating medical treatments in pathological cases. In this sense imaging is an evolutionary domain of measurement techniques with the attractive properties, such as small invasiveness, deep and precise insight into the nature of system. What is more, images are typically much more informative for physicians than pure trends of other signals, e.g. of electrical nature, and direct (visual) disentanglement of information seems also to be easier here. On the other hand, working with this new kind of information stream requires operation on huge sets of data and much more advanced mathematical procedures of signal processing. Usefulness of imaging techniques can be enhanced by designing of original circuits for image acquiring and reconstruction, but vast work should be done also in a range of image transformation in order to extract directly invisible and/or inseparable components and quantify them for decisive reasons. All these could support diagnostic and interventional procedures of medical environment, as a hand-made assessment can bring to a small level of reproducibility even for highly trained readers [1]. Lung diseases are one of the most important factors of statistics devoted to morbidity and mortality around the world [2] [3] [4]. Imaging techniques play an increased role in clinical and research work as in opposite to classical but selective pulmonary function tests, e.g. spirometry [5, 6] or wash-out technique [7], they enable assessment of airway anatomy, regional lung mechanics, and associated lung function (gas exchange) [8]. There are different techniques used for detecting lung pathologies, and among them CT (computer tomography) is very important. Even with HRCT (high resolution computer tomography), not all pathologies are easily detectable; that is, for example, indolent tumors or undetermined significance pathologies related to lung that are difficult to pointing out because of their slow and stealth evolution. It is meaningful that to understand the complexity of the respiratory system, processes governing the respiration and alterations in pathological cases, the system must be examined in the intact dynamic state. Such an examination requires both the spatial and temporal resolution necessary to evaluate details on anatomy (airway and parenchyma) and function (regional delivery of gas or blood along with changes in lung morphometry or parenchymal density) [8] [9]. Recently new imaging techniques are emerging to help us to understand the molecular and cellular aspects of lung health and disease[10]. In the paper, the effort is directed toward original application of Hough transform model to various lung imaging in order to extract its characteristic features. The scope of research is to provide

objective and reliable tool for fast distinguishing of primitives of complex shapes due to potential undetermined significance pathologies. Functional engineering analyses were provided for operation of circular Hough algorithm on medical imaging of various quality, i.e. HRCT, CT, and spiral CT. CT technique is used since it displays good results with respect to MRI for lung tissues [11] [12]. The meaning of various distorted qualities of medical images can be neutralized here thanks to inherent resistance of Hough transform to noisy component and ability to work with occluded shapes. The structures detected should be classified by a measurement of entropy in order to consider only areas with a strong contrast related to a lung disease useful for clinical diagnosis because abnormalities [13-16] in the analyzed images are present as a set of points more lighter in lung image.

II. THEORETICAL ASPECTS OF HOUGH TRANSFORM

In a medical image, the pertinent information about an object is very often contained in the shape of its boundary. The course of edge in a living world typically shows important complexity, which makes an algorithm more advanced and time-consuming, whereas the process of diagnosis imposes on engineers a demand of as quick as possible access to information encoded in source picture.

Popular way of dealing with medical images, especially in computer tomography, is a Radon transform [17]. Introduced in 1917 and newly uncovered for scientific applications after 1960s, this operation converts features from the image space into a parameter space. The Radon transform is a mathematical integral transform defined for continuous functions on, but parameterization for simple geometrical form leads to interesting theoretical and practical results. A straight line in the (x,y) plane is described by

$$y = m \cdot x + b \tag{1}$$

where m is the slope and b is the intercept in the Cartesian coordinate system. Due to the fact that perpendicular lines to the x-axis can give unbounded values for parameters m and b (m and b rises to infinity), lines can be parameterized in polar coordinates, i.e. the length r and the orientation ϑ of the normal vector to the line from the image origin. Thus, a straight line is represented by the following equation [18]:

$$r = x\cos\vartheta + y\sin\vartheta \tag{2}$$

which means that point in a source (image) space is represented by line in a destination (parameter) space, and on the other hand, a line in the (x,y) space is represented by the point

of intersection of sine curves in the characteristic 'butterfly' pattern (Fig.1).

For a general case of a grey-scale intensity function *g(x,y)*, the Radon transform can be rigorously defined as

$$R(r,\vartheta)=\int_{-\infty}^{\infty}\int_{-\infty}^{\infty} g(x,y)\delta(r-x\cos\vartheta-y\sin\vartheta)dxdy \tag{3}$$

where $\delta(\cdot)$ is a Dirac delta function forcing an integration along the straight line described by equation (2). When *g(x,y)* accepts binary values 0, 1 only (black and white), then the line integration comes down to simply counting (or accumulation) of the unit-valued pixels, and equation (3) becomes, in fact, the Hough transform (HT) definition [19]. Summarizing, Hough transform operates on discrete spaces (images) whereas Radon transform was defined as continuous transformation.

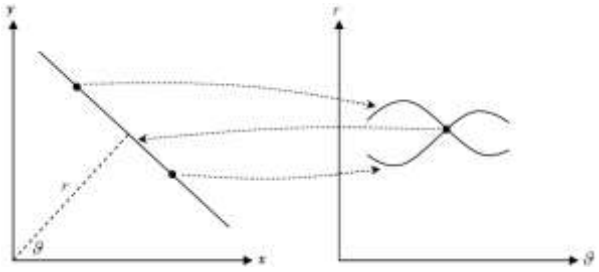

Figure 1. Parametrization of the line in space.

In the simplest form of the Hough transform, i.e. the straight line Hough transform (SLHT), the collinearity of points of the line of Fig. 1 is verified in the parametric space which is defined by accumulator matrix: each feature point votes for a sinusoid of points in the accumulator [20]. Where these sinusoids cross, there are higher accumulator values. Finally, finding maxima in the accumulator equates to finding the lines. The basic Hough transform has been extended to more complex shapes where the regime of parameterization was still used – circular Hough transform (CHT) [20, 21]. But detection of circles and ellipses is connected with higher dimensions (3 or 5) of parameter space and accumulator array. To overcome this drawback the radius can be held as a constant or limited to number of known radii [22]. This has triggered the involvement of interval arithmetic in Hough calculation [23]. What is more, Hough algorithm is often supplemented with information about edge direction in order to reduce the search in the parameter space [24]. In this attempt, the accumulator contains numbers corresponding to the number of circles passing through the individual coordinates, which means that the highest numbers correspond to the centre of the circles in the image [25]. Advancement in designing of Hough transformation was achieved in work of

Ballard [26] who generalized the detection to arbitrary shapes, which cannot be represented analytically. Other direction of works on HT was devoted to decreasing of computational effort resulting from scanning a vast parameter space. It has given the rise to fast Hough transform (FHT) [27], mechanisms of which can be applied in every class of Hough transformation. Some distinct advantages have determined the popularity of Hough attempt in a computer vision domain. First of all, each image point is treated here independently and therefore a parallel processing is possible which enable real time applications. In addition, noisy image points are unlikely to contribute to a peak in the parameter space, which makes this method robust to the presence of noise. Finally, since each image point contributes independently to the parameter space points, the algorithm is able to work even if the shape is occluded. These characteristic properties implicate possible and diagnostically fruitful applications in medical sciences. The adequate examples can be the attempt with segmentation of key bone structures within the pelvis in the X-ray images [28, 29], work devoted to 3D reconstruction of lung movement from MR images [30, 31] or pulmonary artery segmentation in 3-D chest CT [32]. In these examples, HT and CHT play a key role as further and extensive applications especially for MR images. We may know that MR diagnostic is not very useful for static lung characterization but for movement.

III. BIOMEDICAL IMAGE PROCESSING AND PROPOSED ALGORITHM

As illustrated in previous section, Hough transform is a powerful asset to help scientists and researchers to detect edges. Algorithms of the extraction of edges are developed before of the Hough transform. Its rough and quick application, using simple Matlab® instructions, is depicted in Fig. 2 for the case of CT images.

Figure 2. CT of one month child suffering from fever. Localized fibrous tumor of the pleura. Original image (left), binary image and edges of the image (center and right).

One of the most important advantages of Hough transform is to detect lines with short breaks in them due to noise, or when objects are partially occluded. The major disadvantage is that it

can give misleading results when objects happen to be aligned by chance. To overcome Hough transform limitations, especially in diagnosis, it is better to change the problem approach by choosing to circle spots and changes in images by using circular Hough transform as it is shown below. Circular Hough transform [33] detects circular shapes in a grayscale image. The equation of a circle is

$$r^2 = (x-a)^2 + (y-b)^2 \tag{4}$$

where a and b are the centre of the circle in the x and y direction respectively and r is the radius. The parametric representation of the circle is

$$\begin{aligned} x &= a + r\cos(\vartheta) \\ y &= b + r\sin(\vartheta) \end{aligned} \tag{5}$$

The possible minimum and maximum radii of the circles to be searched must be set in pixels units. In this way the problem has a complexity R^2 instead R^3, because the coordinate of the center *(x,y)* and the radius should be known to draw the circle. In this case the range of radii is set and the complexity of the problem is reduced. The algorithm is based on the gradient field of the input image. A threshold on the gradient magnitude is performed before the voting process of the Circular Hough transform to remove the 'uniform intensity'. In other words [34], pixels with gradient magnitudes smaller than the value of threshold are not considered in the computation (the pixels of background which are not important are eliminated by the successive computation while the shapes of more interested objects in the figure are pointed out). Calculating gradient is equivalent to estimation of all edges in the image; the edges of the more interested object in the image. For each edge point, a circle is drawn with center in the point with the desired radius in the parameter space (Fig. 3).

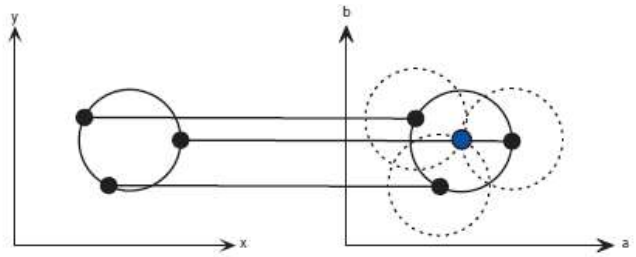

Figure 3. Geometrical transformation due to the application of circular Hough transform from the x,y-space (left) to the parameter space (right); this example is given for a constant radius.

So, in this way we sweep over every edge point in the input image drawing circles with the desired radii and incrementing the values in the accumulator. When every edge point and every desired radius is used, the accumulator is considered. The accumulator will contain

numbers corresponding to the number of circles passing through the individual coordinates. Thus the highest numbers correspond to the center of the circles in the image. To do this, a number of area of interest are selected in the accumulator array and the local maxima are searched. The local maxima candidates are grouped by adjacency [35]. A process of labelling is used to group pixels belonging to same objects and through a principle of 8-connectivity, the adjacent pixels must be selected. For each group the position of the center is calculated, and next it is taken as the center of one circle detected. The radii are estimated and the circles are drawn on the original image. The algorithms proposed for the purposes of this research is shown in Fig. 4. It directly uses the acquired image and no preliminary operations for enhancing the quality of image are implemented. So the circular Hough transform is applied to the image as explained above, and the steps are shown in the block diagram.

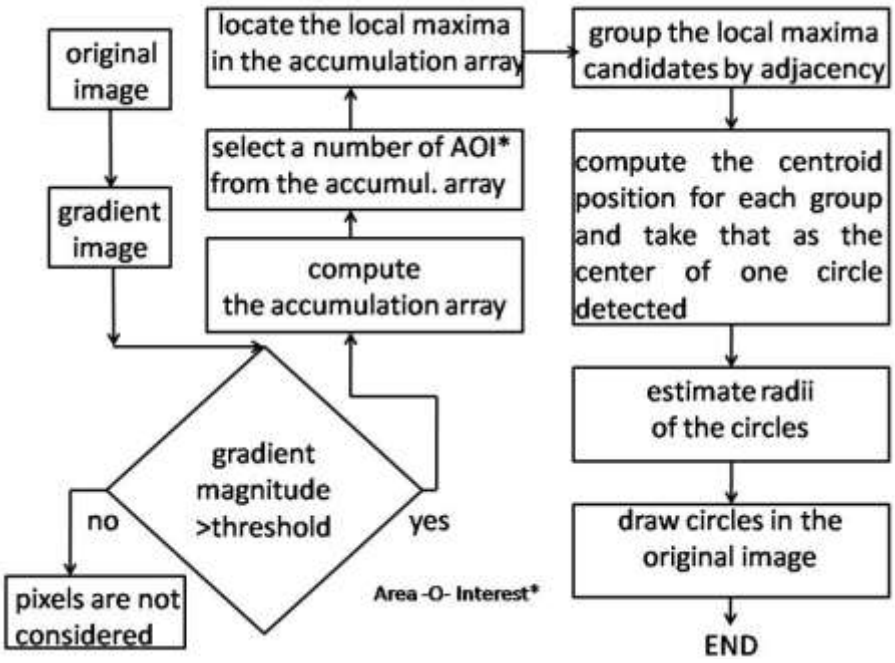

Figure 4. Circular Hough algorithm used in the paper to produce the outcomes of section 4 for different quality of images (HRCT, CT)

It is explained previously, Hough transform identifies in the image the circular shapes which are obtained by the pixels belonging to the edges of the image. An element of the edge is a point of the image where a discontinuity of the gray value occurs. It is possible to see in the Fig. 5, the biomedical images of a patient with lung disease. This image has a strong variability of the levels of gray and so the detected circles through Hough transform can be numerous and in this way it can be very complex to identify abnormalities. The red arrow in Fig. 5 shows one of the areas to be taken into consideration during the diagnosis as it occurs in a different way than the rest of the lung that has a gray level more uniform, and swellings

of the trophic vessels are also visible.

Figure 5. A 26-year-old woman with chronic lung disease presents with significant hemoptysis. The computer tomography could hide AVM (Arterious Venous Malformation) as described in the left.

The very first parameter useful to underline several regions than others is the choice of threshold to compare the magnitude of gradient in the algorithm (Fig. 4). It is good to choose this value not very low because the reduction of the circles with a second parameter allows to control the process in a soft way and to keep the information more important without clear useful details. This second parameter is the entropy. It is an index of the variability of the gray levels in the histogram over the full available range. Knowing the occurrence of L gray levels in an image with the probability of occurrence of the l^{th} gray level $p(l)$, $l=0,1,...,L-1$, a measure of average information or entropy is defined as the expected value of information contained in each possible level:

$$H = -\sum_{l=0}^{L-1} p(l)\log_2(p(l)) \tag{6}$$

To choose the circles produced by Hough transform, we consider a square region which contains the detected circles. In Fig. 6 the outcome of Hough transform is shown, where it is possible to see the innumerable circles defined by the selected radii (14-18 pixels), and a detail of the image over the square region containing the circle.

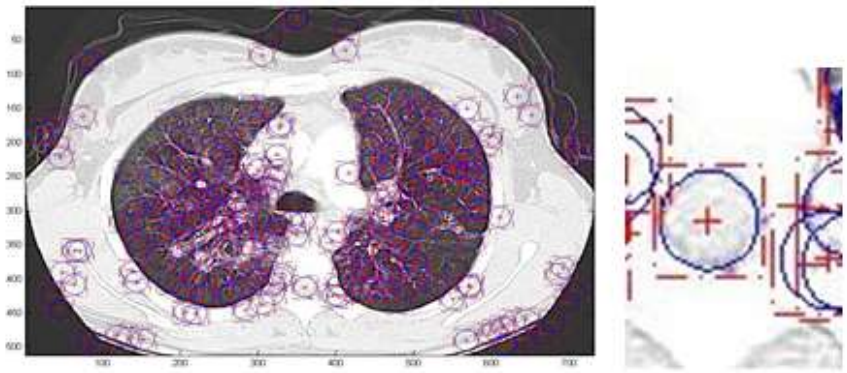

Figure 6. Outcome of Hough transform and its detail

These regions must be selected through a measurement of their entropy: a high value of entropy means all the gray levels occur with the same probability. The number of gray levels in an image is 2^k, so *Hmax* is *k* bits. For the scope of this work, the necessity to detect abnormalities brings to set the range of entropy very high because abnormalities in the biomedical image are characterized by areas with high contrast in the image. The idea is to study the entropy for each region containing one of the circles detected by Hough transform. These regions are of appropriate size to contain, in addition to the circular area of interest, also a certain number of pixels belonging to its surroundings. The square has a dimension *d*+4 pixels * *d*+4 pixels, where *d* is the diameter of the circle. The size has been set as a result of various tests in which it is seen that the amount of pixels taken into account is sufficient to define the contrast of detail related to the pathological condition of the patient with respect to the rest of the area identified instead as a normal one.

IV. RESULTS

The algorithm of Fig. 4 has been applied for detecting further medical items in CT and HRCT images. Each medical image is related to a specific respiratory diagnosis. The first image analyzed is in Fig. 5. At the beginning of the algorithm, the range of the radii of the circles to search in the image is set. For example, the circles with a radius of 8-10 pixels must be searched. Then the gradient image is calculated and the pixels under the threshold chosen are not considered. The value of threshold is selected in a way to keep the useful information in the image, so the histogram of the gradient image helps to set an appropriate value.

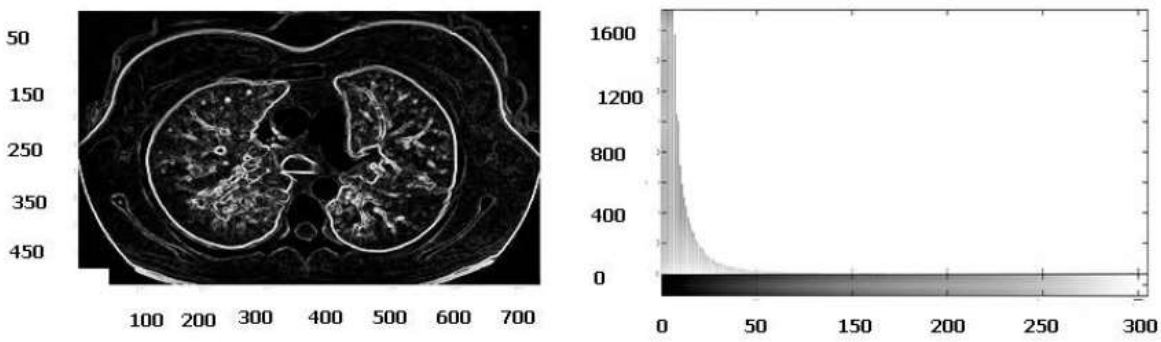

Figure 7. Gradient image and its histogram of CT image

In this case, a value of 7 allows to remove the uniformity distribution due to background and related to objects with a low discontinuity. So with this candidates pixels the accumulator array is calculated (Fig.8), and the following map of local maxima is obtained (Fig.9):

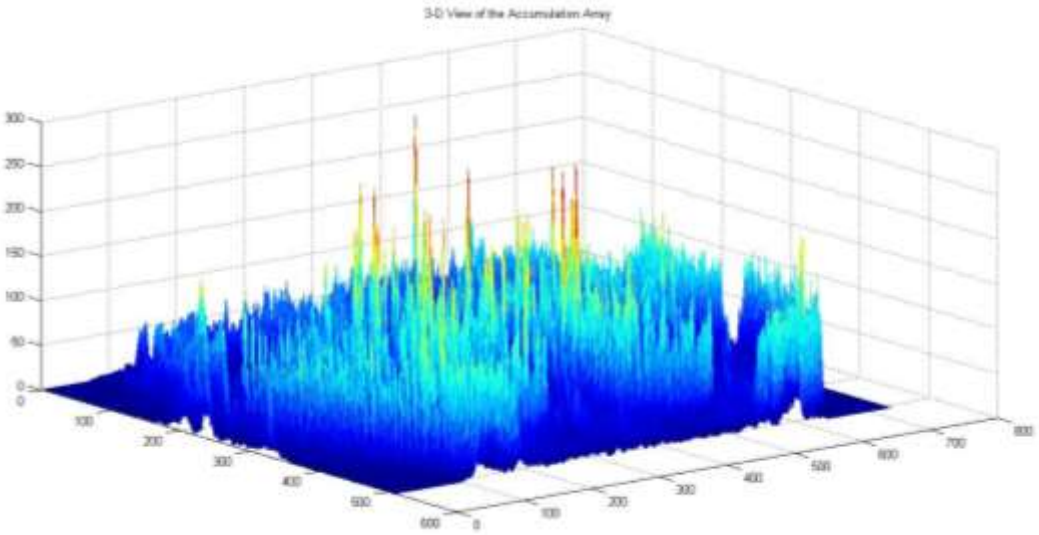

Figure 8. Array Accumulator of CT image

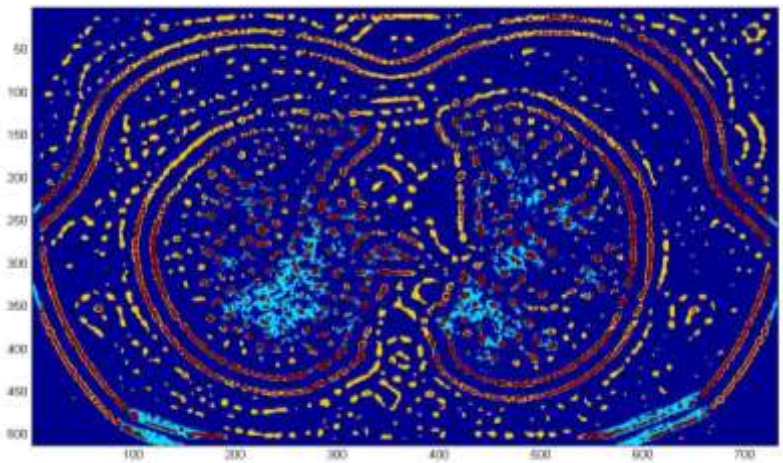

Figure 9. Generated map of local maxima of CT image

A process of labeling is applied to group the pixels related to the same object. The adjacent pixels are selected through a 8-connettivity principle. The output of Hough transform is shown in Fig. 10. The Hough transform detects accordingly a large number of circles with desired radius; moreover, Hough transform detects structures in the image which are not visible thanks to its capability to perform geometrical transformations.

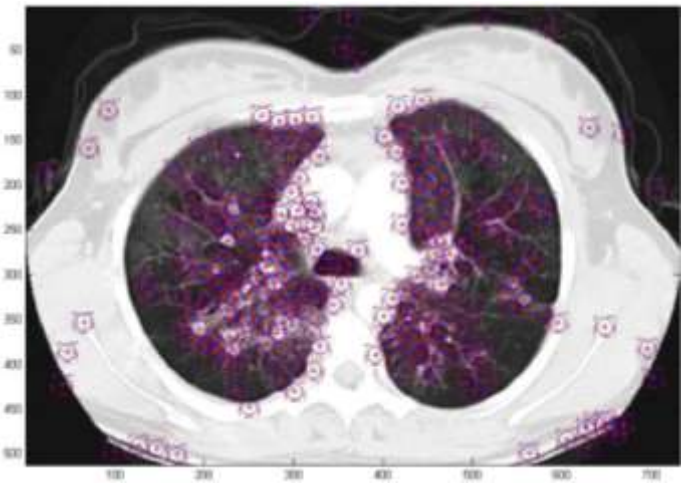

Figure 10. Hough transform applied to the CT image

But it is necessary to reduce the significant circles only to the objects of interest which could emphasize any abnormalities in the organ under observation. In this sense, entropy is useful because it allows to focus the attention on regions with high contrast and to reject circle without interest. The entropy-based detection acts according to two ways: low entropy values produce low frequencies, hence we can see uniform regions of the considered images; analogously, high entropy values imply high frequencies that bring to image edges. Fig. 11 shows the entropy, in function of number of circles, calculated for each detected circle by Hough transform. As it is previously sentenced high values of entropy yield to detecting edges, in our case points that are different from the rest of the image. Values of entropy ranging between 6 and 7, envisaged interval, allows to see different interesting points which the clinicians can pay attention on. That is the range that is useful for the interpretation. It shows the chosen range to select the circles of interest. This range is set between max value entropy and the 10% of its value (better best range chosen on the base of different tests to avoid to lose useful information).

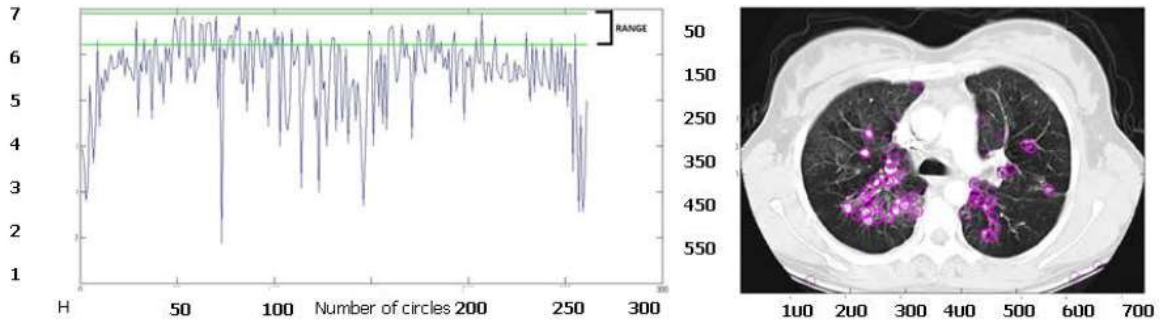

Figure 11. Entropy (left) calculated for each detected circle with Hough transform in CT image and the outcome (right) obtained after the selection of the circles related to the indicated range of the entropy.

The image on the right in Fig. 11 reports the result obtained after the application of the entropy measurement (see ordinates axis) with respect to the number of circles (abscissa). As it is possible to see, only circles that have high values of gray, compared to the rest of the image which is dark, are preserved. Again, going back to Fig.11, it is instructive to see, by the definition of entropy, the trend looks like a set of compact spikes ("similar to compressed accordion"); this means a high number of close circles with some superpositions as it is illustrated in the right side of Fig.11. In a similar way the process is applied on HRCT image of Fig. 12, obtaining the results of Figs.13 and 14.

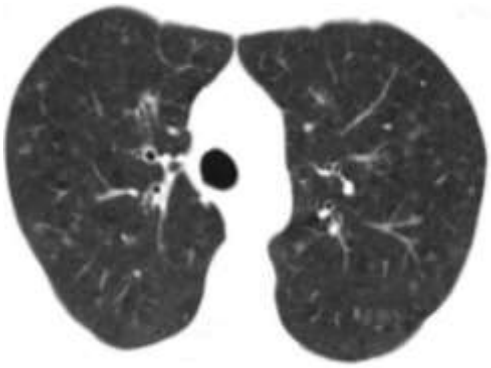

Figure 12: A 40-year-old woman presents with cough and progressive shortness of breath. She has a significant history of smoking.

The combination of Hough transform with entropy gives good results for the case of HRCT images too. In fact, the lung disease is pointed out by enlarged trophic vessels characterized by a shade of gray near to white as it is possible to see in Fig. 12.

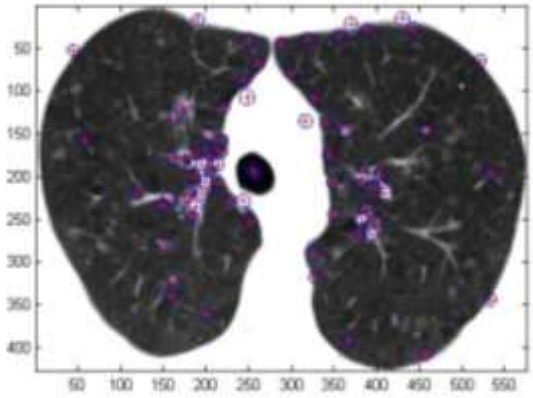

Figure 13. Outcome obtained by only using Hough Transformer

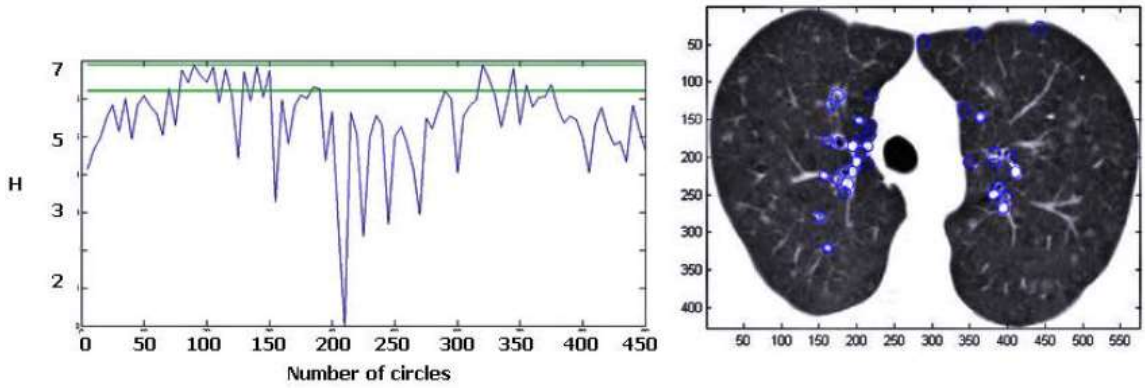

Figure 14. Entropy (left) calculated for each detected circle with Hough transform and the outcome (right) obtained after the selection of the circles related to the indicated range of the entropy.

Analogously, as we can see in Fig.14 (left), using the same range, in order to make a clear comparison, relaxed and reduced spikes ("similar to stretched accordion") display a low number of circles as it is indicated in Fig.14 (right). The algorithm proposed in this article allows to identify these areas more or less in automatically way. Of course, particular attention must be paid in the setting threshold values of the gradient of entropy since they are the main parameters on which it is possible to classify the areas of interest. In the future, these parameters must be investigated more accurately so that they can be chosen in a manner substantially automatic. It is clear that the choice of the range of entropy influences the region of convergence (ROI). As a matter of fact, we have processed 4 images for CT and as much for HRCT. NMR (nuclear magnetic resonance) is not indicated for lung apparatus. In order to be coherent, as it is mentioned in the beginning, we should compare CT with HRCT. A summary of results is illustrated below since 3 experts have been called to detect the number

of suspected points (circles) and their sizes. The results are shown in Table 1. For sake of shortness, we use two images, that are Fig.10 as CT and Fig. 13 as HRCT. In both situations we utilize normal Hough based algorithm and an enhanced version with entropy. Only in case of entropy implementation we have a coincidence between experts'detection of point numbers and the algorithm results. That is the gold standard. But in case of normal Hough algorithm, even there is still a consensus among the expert, the algorithm produces a point numbers three times than the expected one. This is due to the presence of points and contours included in the images that have a different tonality. Moreover, thanks to Hough algorithm-based entropy, the experts have improved the interpretation by reformulating the diagnosis as it is illustrated in Fig.15 where we can see the different between the concise interpretation of American College of Radiology and that performed by our experts. Entropy subtechnique is more accurate than classical Hough one.

Table 1. Number of circle detection by 2 clinicians and CT expert and the proposed algorithm. *orig*, *ne*, and *we* stand for original, no entropy and with entropy respectively. Sizes are in mm.

Fig	Det.#	Observer#1			Observer#2			Observer#3			Algorithm		
		left	right	size	left	right	size	left	right	size	left	right	size
10 CT	1 (orig)	35	21	2-3	34	20	2-3	33	20	2-3	-	-	-
	2 (ne)										110	74	2-2.5
11 CT	1 (orig)	35	21	2-3	34	20	2-3	33	20	2-3	-	-	-
	2 (we)										33	20	2-2.5
13 HRCT	1 (orig)	20	14	3-4	19	14	3-4	19	14	3-4	-	-	-
	2(ne)										37	34	2-2.5
14 HRCT	1(orig)	20	14	3-4	19	14	3-4	19	14	3-4	-	-	-
	3(we)										19	14	3-3.5

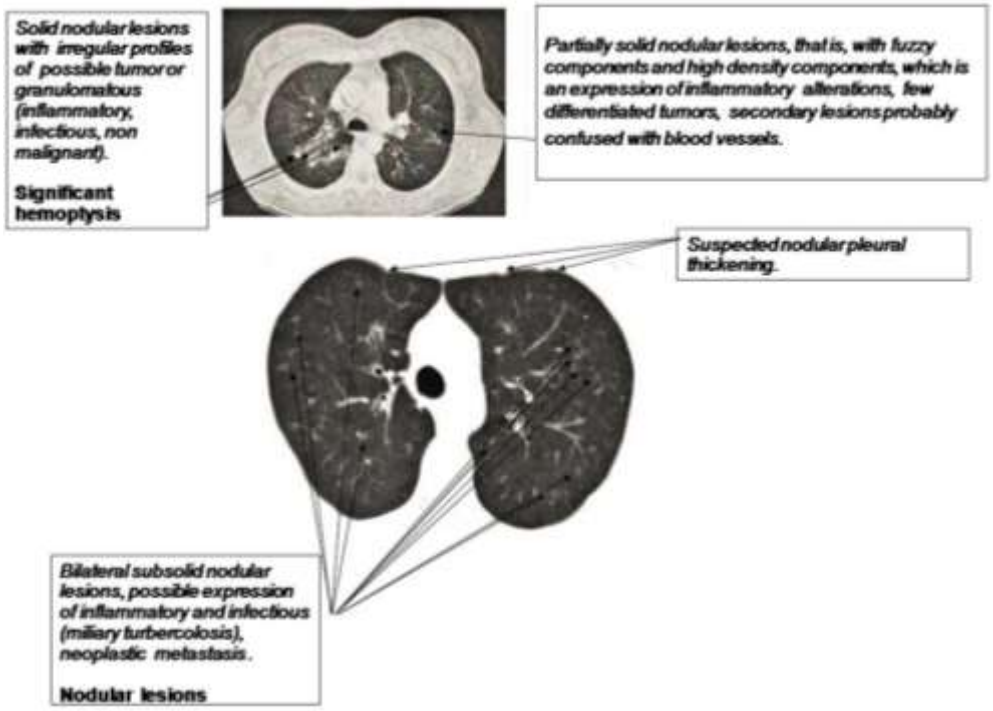

Figure 15. Interpretation after the algorithm based on entropy. Captions in italics means the interpretation after entropy-based algorithm while normal bold captions are related to the original diagnosis. Upper image: related to Fig.11. Lower image: related to Fig. 14.

Beyond the results displayed in Table 1, we also used another parameter as a parameter of improvement called receiver operational curve (ROC). ROC is an index of accuracy [36]; it is a curve that represents, in ordinates, the proportion of positive tests within sick population (sensitivity) in function of the proportion of positive tests among non sick population (specificity in abscissas), for all threshold values of test. For the cases of this research, the threshold is related to the number of spots (circles) on the images established by the experiences of the operators of Table 1. Two sets of previous images (Fig.10, Fig.11) and (Fig.13,Fig.14), that illustrate the situation before and after entropy application, are processed using a well-known free software called MedCalc® [37]. This software is robust and allows different other elaborations. Figures are divided in useful small grids (area) for allowing the calculation of ROC, determining a number of equal areas and spots per area. Un index of tumor mass, related to each area, is computed where one or more spots (circles) are present, according to

$$index = \frac{Number\ of\ spots\ x\ number\ of\ spots\ per\ area}{square\ area} \tag{7}$$

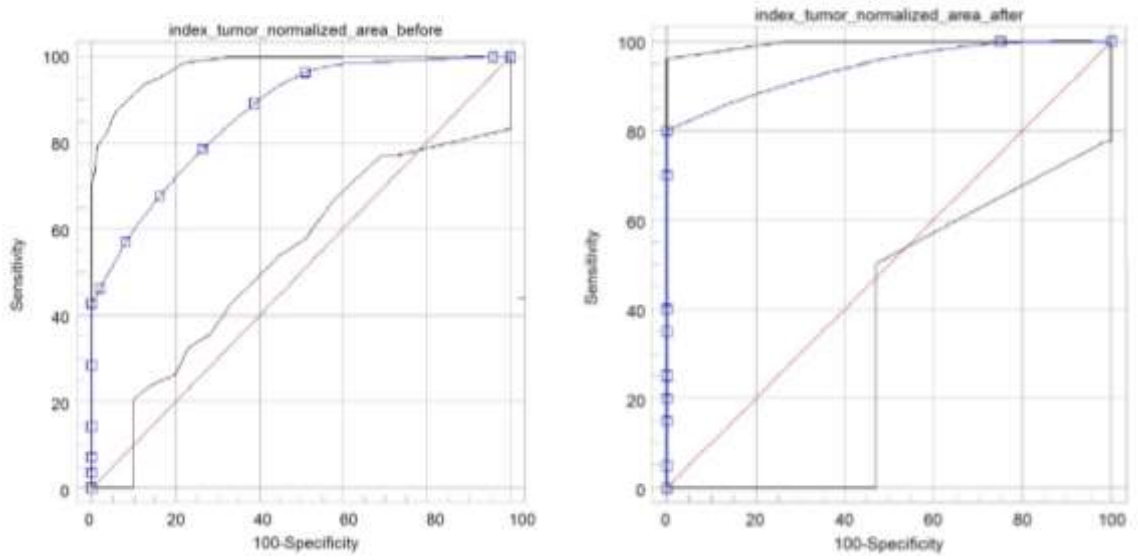

(a) (b)

Figure 16. Determination of ROC for Fig.10 (left, before entropy) and Fig.11 (right, after entropy application).

Afterwards, a setting is performed as "0" for areas where spots disappear during from "before" and to "after" and as "1" for areas where spots remain or decreasing from "before" and to "after". That is done in accordance with physicians. For diagnosis, areas with high concentration of spots have to be considered as "areas with high index of tumor mass". Fig. 16 (b) and Fig.17 (b) illustrate the improvement of the diagnosis by using entropy approach. That is a confirmation of the proposed theory.

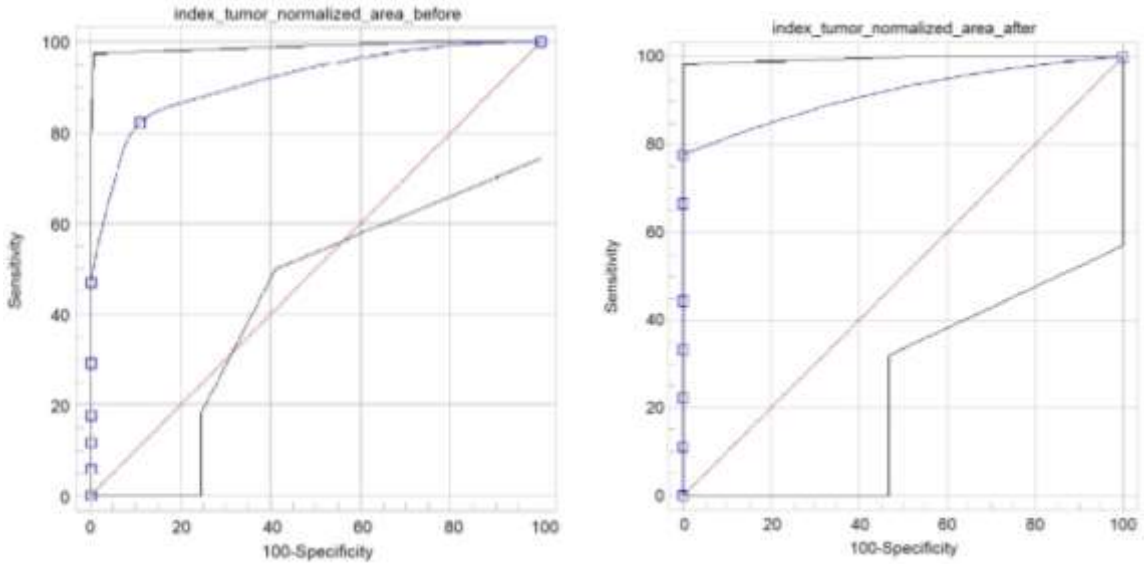

(a) (b)

Figure 17. Determination of ROC for Fig.13 (left, before entropy) and Fig.14 (right, after

entropy application).

V. CONCLUSIONS

Early detection of lung disease in order to obtain a reduction in mortality and the use of automatic image analysis is very useful for interventional radiologists who must only formulate the diagnosis on the basis images, the majority of which corresponds to a non-chronic patients. In this paper we have presented a useful approach of CT and HRCT –based biomedical images of people suffering from lung diseases. The approach is economically cheaper than those using other techniques using nanoparticles [38] and segmentations [39] for better targeting the region of interest. These anomalies occur in the lung as bulges of trophic vessels and so they are characterized by circular shape with a gradation of gray closer to white. The problem is that even these areas may be visible to the naked eye, but sometimes the smallest details may be obscured as for indolent tumour. For example, in the image of Fig. 5 the right lung area which presents a pathological structure immediately visible obscures the left part where there are abnormalities also. These regions are highlighted by the final result of the proposed algorithm as shown in Fig.11 where the circles obtained by the combination of the Hough transform and by a measurement of the entropy show further areas to keep under control. However, improvements are needed in the setting of the threshold values of the gradient on which the Hough transform is calculated and entropy for classifying areas of interest in order to have a higher accuracy in the areas to be located. Even there are other algorithms that can be applied for circumstances of the present research, we do believe that Hough combined with entropy is a quick and a robust algorithm. This fact is demonstrated by the points of the lower image of Fig.15 where the algorithm has stimulated the experts to detect a suspected nodular pleural thickening which is generally an indolent tumour of difficult detection. The proposed algorithm could suffer from an excess of pointing out abnormalities on image but it is an acceptable result since it compels the expert to pay more attention even this aspect represents a loss of time. However, treating with pathologies, especially with tumour, a loss of time is acceptable for saving people'life. Moreover, the use of ROC has pointed out the accuracy of entropy subtechnique as it is illustrated in Fig. 16 (a,b) and Fig. 17 (a,b). As a matter of fact, the accuracy in detection depends upon the quality of biomedical sensing system that must be in line with severe requirements [40] and the spectrum of the system. In some cases, thermal imaging with special configurations [41] is able to overcome some (but not all) limitations due to hidden tissues.

Acknowledgments

Authors gracefully acknowledge the American College of Radiology for allowing the use of images for the scope of this research and they state : " *Reprinted with permission of the American College of Radiology. No other representation of this material is authorized without expressed, written permission from the American College of Radiology*". They thank the hospital clinicians Francesco Biancofiore (R.I.P), who recently has departed and Sergio Agati, and the interventional radiology expert Luigi De Feo for their help in medical interpretation issues. A special thank is tributed to Prof. Francesco Lamonaca for discussions in Hough Transform for lung imaging.

REFERENCES

[1] N.A. Jarad, P. Wilkinson, M.C. Pearson, R.M. Rudd, "A new high resolution computed tomography scoring system for pulmonary fibrosis, pleural disease and emphysema in patients with asbestos related disease", Br. J. Ind. Med. Vol. 49, N.2, pp. 73-84.

[2] I. Jabłoński, "Properties of occlusional devices in extended time-frequency analysis of post-interrupter respiratory signals", IEEE Sensors J., Vol. 12, N.3, pp. 504 – 511, 2012.

[3] S. Urooj, M. Khan, Aq Ansari, A. Lay-Ekuakille, A.K. Salhan, "Prediction of Quantitative Intrathoracic Fluid Volume to Diagnose Pulmonary Edema Using Labview", Computer Methods in Biomechanics and Biomedical Engineering, Vol. 15, N. 8, August 2012, 859–864, 2011.

[4] A.Lay-Ekuakille, G. Vendramin, A. Trotta, "Spirometric Measurement Post-Processing: Expiration Data Recovery", IEEE Sensors Journal, Vol.10, n.1, pp.25-33, IEEE Sensors Journal, 2010.

[5] U. Frey, P.J.F.M. Merkus (Eds.), "Paediatric lung function, European Respiratory Monograph", European Respiratory Society, Vol. 47, pp.1-31, 2010.

[6] R.E. Dales, K.L. Vandemhen, J. Clinch, A.D. Aaron, "Spirometry in the primary care setting. Influence on clinical diagnosis and management of airflow obstruction", Chest., Vol. 128, N.4, pp. 2443-2447.

[7] S. Loom et al., "Early detection of cystic fibrosis lung disease: multiple-breath washout versus raised volume tests", Thorax. Vol. 62, N. 4, pp. 341–347, 2007.

[8] M. Castro, "Lung imaging in asthmatic patients: the picture is clearer, J. Allergy Clin. Immunol.", Vol.128, pp.467-478, 2011.

[9] A. Lay-Ekuakille,P. Vergallo, A. Trabacca, M. De Rinaldis, F. Angelillo, F. Conversano, S. Casciaro, "Low-Frequency Detection in ECG Signals and Joint EEG-Ergospirometric Measurements for Precautionary Diagnosis", Measurement, Vol. 46, N. 1, pp 97-107, 2013.

[10] Y. Cui, B. Zhao, T.J. Akhurst, J. Yan, L.H. Schwartz, "CT-guided automated detection of lung tumors on PET images", Proc. of SPIE, Vol. 6915, Feb 19-21, 2008.

[11] J. L. Mulshine, "Screening for lung cancer: in pursuit of pre-metastatic disease", Nature Reviews Cancer, Vol.3 pp.65-73, January 2002.

[12] S. Brandman, Jane P. Ko, "Pulmonary Nodule Detection, Characterization, and Management With Multidetector Computed Tomography", J Thorac Imaging, Vol. 26, n. 2, pp.90-105, May 2011.

[13] F. Conversano, A. Greco, E. Casciaro, A. Ragusa, A. Lay-Ekuakille, S. Casciaro, "Harmonic Ultrasound Imaging of Nanosized Contrast Agents for Multimodal Molecular Diagnoses", IEEE Transactions on Instrumentation & Measurement, Vol.61, N. 7, pp. 1848-1856, 2012.

[14] S. Casciaro, F. Conversano, L. Massoptier, R. Franchini, E. Casciaro, A. Lay-Ekuakille, "A Quantitative and Automatic Echographic Method for Real-Time Localization of Endovascular Devices", IEEE Transactions on Ultrasonics, Ferroelectrics, and Frequency Control, Vol. 58, n.10, pp. 2107-17, 2011.

[15] F. Conversano, R. Franchini, S. Casciaro, A. Lay-Ekuakille, "In Vitro Evaluation and Theoretical Modelling of the Dissolution Behaviour of a Microbubble Contrast Agent for Echographic Imaging", IEEE Sensors Journal, vol.12, n.3, pp. 496-503, 2012.

[16] G. Soloperto, F. Conversano, A. Greco, E. Casciaro, A. Ragusa, A. Lay-Ekuakille, S. Casciaro, "Assessment of the Enhancement Potential of Halloysite Nanotubes for Echographic Imaging", IEEE MEMEA 2013, may 4-5, 2013, Canada.

[17] F. Natterer, E.L. Ritman, "Past and future directions in X-ray computed tomography (CT)", Int. J. Imaging Syst. Technol., Vol. 12, N.4, pp.175–187, 2002.

[18] R.O. Duda, P.E. Hart, "Use of the Hough transformation to detect lines and curves in pictures", Comm. ACM. Vol. 15, N.1, pp.11-15, 1972.

[19]V.A. Shapiro, V.H. Ivanov, "Real-time Hough/Radon transform: algorithm and architectures"; in proceedings of the International Conference on Image Processing, November, 13-16, Austin USA, 1994.

[20] D. Antolovic, "Review of the Hough transform method with an implementation of the fast Hough variant for line detection", htpp://www.cs.indiana.edu/ftp/techreports/TR663.pdf., Indiana University, 2008.

[21] J. Lladós, "The Hough transform as a tool for image analysis", http://citeseerx.ist.psu.edu/viewdoc/summary?doi=10.1.1.8.469.

[22] D.B.L. Bong, K.H. Lim, "Application of fixed-radius Hough transform in eye detection", Int. J. Intell. Inform. Technol. Appl. Vol. 2, N.3, pp. 121-127, 2009.

[23] R.Y. Takimoto et al., "Detecting function patterns with interval Hough transform"; in proceedings of 9th IEEE/IAS International Conference on Industry Applications (INDUSCON), São Paolo, Brazil, November, 8-10, 2010.

[24] J. Illingworth, J. Kittler, "A survey of the Hough transform", CVGIP, Vol.44, N.1, pp. 87-116, 1988.

[25]S.J.Kjelgaard Pedersen, "Circular Hough transform", http://www.cvmt.dk/education/teching/e07/MED3/IP/Simon_Pedersen_CircularHoughTransform.pdf, November 2007.

[26] D.H. Ballard, "Generalizing the Hough transform to detect arbitrary shapes", Pattern Recogn., Vol. 13, N. 2, pp. 111–122, 1981.

[27] H. Li, M.A. Lavin, R.J. LeMaster, "Fast Hough Transform: a hierarchical approach", CVGIP., Vol.36, N. 2-3, pp.139-161, 1986.

[28] R. Smith, K. Najarian, K. Ward, "A hierarchical method based on active shape models and directed Hough transform for segmentation of noisy biomedical images; application in segmentation of pelvic X-ray images", BMC Med. Informatics and Decision Making. Vol.9, N.1, Suppl 1:S2, 2009

[29] S. Hu, E.A. Hoffman, J.M. Reinhardt, "Automatic lung segmentation for accurate quantitation of volumetric X-ray CT images", IEEE Trans. Med. Imag. Vol. 20, N. 6, pp. 490-498, 2001.

[30] R.S. Tavares et al., "Lung movement determination in temporal sequences of MR images using Hough transform and interval arithmetics"; in proceedings of the 7th IFAC Symposium on Modelling and Control in Biomedical Systems, August, 12-14, Aalborg, Denmark, 2009.

[31] R.S. Tavares et al., Temporal segmentation of lung region MR image sequences using Hough transform; in proceedings of 32nd Annual International Conference of the IEEE EMBS, August 31-September 4, Buenos Aires, Argentina. (2010).

[32] M. Feuerstein, T. Kitasaka, K. Mori, "Adaptive model based pulmonary artery segmentation in 3-D Chest CT"; in proceedings of SPIE Medical Imaging, February 2010, San Diego USA.

[33] M.S. Nixon, A.S. Aguado, "Feature extraction and image processing", II Edition, University of Southampton, 2008, UK.

[34] M. Rizon et al., "Object detection using circular Hough Transform", American Journal of Applied Sciences. Vol. 12, pp.1606-1609, 2005.

[35] D.G. Lowe, "Object recognition from local scale-invariant features", in proceedings of Computer vision Conf., Kerkyra, Greece, 1999.

[36] T. A. Lasko, J.G. Bhagwat, K.H. Zou, L. Ohno-Machado, "the use of receiver operating characteristic curves in biomedical informatics", Journal of Biomedical Informatics, Vol.38, pp. 404–415, 2005.

[37] https://www.medcalc.org/manual/roc-curves.php

[38] F. Conversano, A. Greco. E. Casciaro, S. Casciaro., A. Lay-Ekuakille, "A Novel Dual-Frequency Method for Selective Ultrasound Imaging of Targeted Nanoparticles", IEEE Sensors Conference, Limerick, Ireland, 2011.

[39] S. Casciaro, L. Massoptier, F. Conversano, A. Lay-Ekuakille, E. Casciaro, R. Franchini, R. Verrienti, A. Malvasi, "Fully Automatic Segmentations of Liver and Hepatic Tumors from 3-D Computed Tomography Abdominal Images: a new adaptive initialization method", IEEE Sensors Journal Special Issue on Sensors for Non-Invasive Physiological Monitoring, Vol.12, N. 3, pp. 464-473, 2011.

[40] V. Bhateja, A. Kalsi, A. Shrivastava and A. Lay-Ekuakille, "A Reduced Reference Distortion Measure for Performance Improvement of Smart Cameras," IEEE Sensors Journal, Special Issue on "Advancing Standards for Smart Transducer Interfaces",Vol.15, n.5, pp. 2531 – 2540, 2015.

[41] A. Lay-Ekuakille, P.Vergallo, F. Conversano, S. Casciaro, D. Veneziano, "Thermal Image Processing for Accurate Realtime Decision Making in Surgery", 2014 IEEE MeMea, June, 11-12, 2014, Lisbon, Portugal.